

# Modeling and RST Position Controller of Rotary Traveling Wave Ultrasonic Motor

M.Brahim, I.Bahri, Y.Bernard

GeePs | Group of electrical engineering - Paris

UMR CNRS 8507, CentraleSupélec, Univ Paris-Sud, Sorbonne Universités, UPMC Univ Paris 06

11 rue Joliot Curie, Plateau de Moulon F91192 Gif sur Yvette CEDEX

Mouhanned.brahim@geeps.centralesupelec.fr

**Abstract**— Nowadays piezoelectric motors become alternative actuators to the electromagnetic motors especially for precise positioning applications. Nevertheless, suitable model as precise controller need to be developed to achieve high precision levels. This paper deal firstly with the design of an original model of the rotary ultrasonic motor USR60 from Shinsei. Secondly, the syntheses of precise RST based position controller. The performance of the model and the position controller are evaluated in the MATLAB Simulink environment.

**Index Terms**—USM, TWUSM, piezoelectric motors, RST, discrete time.

## I. INTRODUCTION

Ultrasonic Motors (USMs) offer an attractive solution for micro-positioning applications based on many proprieties: high torque to mass ratio, high torque-low speed capability and braking without supply [1]. Therefore, while gearing is often used with electromagnetic motors, it becomes useless in case of USM. This leads to reduced system complexity, lower failure rates and lightweight applications [2].

The Traveling Wave Ultrasonic Motor (TWUSM) is a special type of motor, which is driven by the ultrasonic vibration force of piezoelectric materials. Flexural wave will be generated at the surface of stator and it's able to rotate the rotor strongly pressed to it [3].

Due to the special structure and the operating principle of USMs, its output characteristics vary according to temperature, pre-pressure, driving frequency, and load torque [2]. Therefore, to fully implement its potential performances, closed loop operation mode is often desired. In order to validate the performance of TWUSM in closed loop system, two aspects need to be satisfied. One is the establishment of an appropriate model about the TWUSM characteristics and control variables (voltage amplitude, frequency, and phase difference). The other one is to develop an accurate and robust controller in front of the nonlinear behavior of the motor and perturbations.

A very good introduction to the construction and operating principle of TWUSM was undertaken in [1]. In these studies, the motor is modeled by an equivalent electrical network of capacitors, resistors, inductors and Zener diodes. In addition to the Equivalent Circuit Model (ECM), analytical models were proposed in [4]. However the developing analytical models did not take the structural characteristic details of the motor into consideration. Finite Element Method (FEM) models have been reserved firstly to USM stator design to determine

the natural frequency of the motor and to analyze the contact interface and the interaction stator/rotor [5]. The time consumption of FEM for parameters analysis makes these models not convenient for control implementation. Working principle and mathematical modeling of TWUSM have been presented in [6]. Interesting attempt to create hybrid models of USM was studied in [7] [8].

In parallel with TWUSM models, different control methods appeared in the literature [14-19]. The most used control variable was the driving frequency because it's the simplest method. □ The main disadvantage of this control method is that the motor is controlled at frequencies above the resonance frequency as the operation of the motor at or below the resonance frequency is unstable when using this control method [3]. Focusing on the position control of USM, this has been also widely reported in research works. These techniques can be generally classified into five categories: PID controller with fixed and variable gains [12-13], adaptive controller [14-15], Fuzzy Logic (FL) controller [16], Neural Network (NN) controller [17], and mixed controller [18-19]. The PID controller is simple and easy to be implemented it suffers from the lower bandwidth and the risk of system instability. With NN and FL controller better accuracy can be obtained. However, USM behavior and parameters variation yields to the growth of network's complexity for the NN controller which will increase the time execution and learning procedure [2]. The FL control is based on the knowledge of USM state and experimental data to make up the fuzzy interference rules. But under certain conditions the motor parameters are variable and the output motion can be outside the interference rules [2]. Adaptive control techniques gave relatively advantageous results with USMs when they are designed based on accurate models.

To overcome the problems listed above, accurate models of USR60 associated to a precise RST position control are proposed. In section 2, the modeling procedure of the TWUSM (USR60) is detailed. This model is based on the electromechanical equations defining the USM working principle, and taken into account the nonlinear behavior of the motor. While the voltage phase difference can be used as control variable, the operation of the motor on the two rotation directions is ensured in this model via this variable. The obtained model can be then easily controlled via the three control variables (voltage amplitude, frequency, and phase

difference). In section 3, RST based position controller is established. The controlled is designed in discrete-time domain for constant and variable position trajectories. It gives the possibility to ensure separately the regulation dynamic and perturbations rejection dealing to a precise and robust controller. The precision of this controller with USMs in presence of load torque ( $T_L$ ) is guaranteed with position error amount of 6% ( $T_L=0.5\text{N.m}$ ). Finally, fast closed loop system without instability is obtained.

The model and the controller are implemented and validated in the MATLAB Simulink environment.

## II. MODELING OF TRAVELING WAVE ULTRASONIC MOTOR

In this section, control model for the rotary TWUSM from Shinsei (figure 1) will be presented. This model will take into account the nonlinear behavior of the motor and will be also suitable for control implementation.

### A. Principle of operation

The cutaway view of the Shinsei TWUSM (USR60) is shown in figure 1(a) [1]. The stator consists of piezoelectric ceramic and elastic body. The rotor is made from bronze material and pressed against the stator. Two sinusoidal waves with a phase shift of  $\phi$  supplies two orthogonal modes of piezoelectric ceramic of USM. Elliptical waves occur on the stator surface as described in figure 1(b):

$$\begin{aligned} V_A &= V_{\max} \sin(2\pi f) \\ V_B &= V_{\max} \sin(2\pi f + \phi) \end{aligned} \quad (1)$$

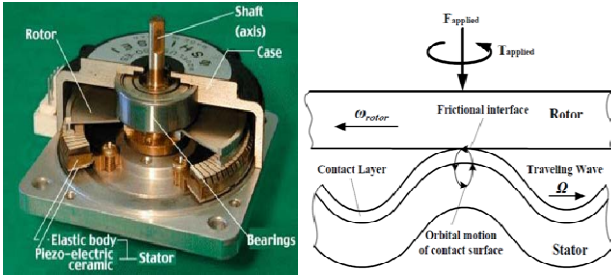


Fig.1: (a) Cutaway view of Shinsei's USR60 TWUSM, (b) Elliptical motion of the stator

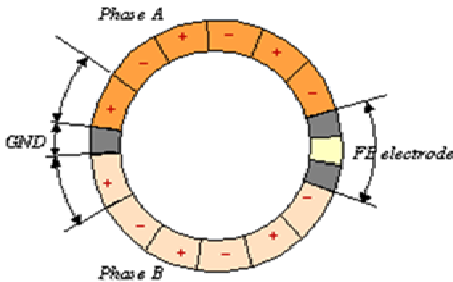


Fig.2: disc and electrode arrangement of USM

The rotor is driven by the tangential force resulting from the elliptical motion at the wave crests. The rotation direction of rotor is opposite to the direction of the traveling wave [10].

As shown in figure 2, piezoelectric ceramics with opposite polarization are placed consecutively so that one will expand while the other will contract when a voltage is supplied. The expansion and contraction of the ceramics causes a transverse traveling wave on the mean plane of the elastic body, which produces elliptical motion of the surface points. Feedback electrode is mounted in addition to the A and B sections. This electrode produces high frequency AC voltage when mechanical vibrations acting on the stator surface. The value of this voltage is proportional to the amplitude of the traveling wave excited in the stator [2].

### B. Modeling concept

The main idea of the modeling procedure of USM is to provide an accurate model which describes: the deformation of the stator and the traveling wave generation, the contact interface stator/rotor, and the dynamic response of the rotor and torque generation. This model will also take into account the nonlinearity behavior of the motor, the effect of load torque and temperature variation. The originality of this model is that the two rotation directions can be ensured using negative and positive values of voltage phase difference ( $\phi$ ). Therefore the motor control via the voltage phase difference can be easily realized. In addition, the motor can be controlled via the voltage supply amplitude ( $V_{\max}$ ), and frequency ( $f$ ),

The motion equations of the stator can be written as following:

$$\begin{aligned} M_{\text{eff}} \ddot{\xi}_1 + C_{s1} \dot{\xi}_1 + K_{s1} \xi_1 &= \eta V_{\max} \sin(2\pi f t) + F_{fs1} \\ M_{\text{eff}} \ddot{\xi}_2 + C_{s2} \dot{\xi}_2 + K_{s2} \xi_2 &= \eta V_{\max} \sin(2\pi f t + \phi) + F_{fs2} \end{aligned} \quad (2)$$

Where:  $M_{\text{eff}}$ ,  $C_{s1,2}$ ,  $K_{s1,2}$ , and  $\eta$  are the effective mass, damping, spring coefficient, and piezoelectric force factor of the stator.  $F_{fs1,2}$  are the feedback forces generated by the stator, and  $\mu$  is the piezoelectric force factor. The amplitudes of the two standing waves are used to calculate the Traveling Wave (TW) amplitude as:

$$\xi_{\max} = \sqrt{\xi_1^2 + \xi_2^2} \quad (3)$$

The TW amplitude will be used then to determine the contact surface between stator and rotor and the angular velocity of the rotor. The feedback force generated by the stator ( $F_{fs1,2}$ ) depends on the contact surface stator/rotor parameters. Therefore, it must be defining those parameters in advance. The most important parameters of the contact surface that should be known are the half contact length ( $X_{H-L}$ ) and the stick point ( $X_s$ ) as shown in figure 3. The half-contact length is defined as half of the horizontal length of the traveling wave crest of the stator submerged within the rotor from its point of entry to its exit. While, the stick points are defined as the location where the horizontal velocity component of the stator surface point matches the horizontal velocity of the rotor, and their magnitude represents the length from the traveling wave crest to that location (Fig.3). The two variables depend on the amplitude of the TW and can be calculated as following [7]:

$$X_{H-L} = \frac{1}{k} \arccos\left(\frac{h(t) - z(t)}{\xi_{\max}}\right) \quad (4)$$

$$X_s = \frac{1}{k} \arccos\left(\frac{R_o^2 \Omega}{k \cdot h \cdot w \cdot \xi_{\max}}\right) \quad (5)$$

Where:  $k$ : is the wave number  
 $h$ : is the half thickness of the stator  
 $z$ : is the vertical distance between stator and rotor  
 $R_o$ : is the effective radius of the traveling wave  
 $\Omega$ : is the angular velocity of the rotor  
 $w$ : is the excitation frequency (rad/s)

The feedback force is composed of normal and tangential components and can be written as function of the half contact length as following [7]:

$$F_{fs,N1,2} = -nC_L \xi_{1,2} (kX_{H-L} - \frac{1}{2} \sin(2kX_{H-L})) \quad (6)$$

$$F_{fs,T1,2} = 2n\mu C_L h \xi_{2,1} (\frac{1}{2} kX_{H-L} + \frac{1}{4} \sin(2kX_{H-L}) - \sin(kX_{H-L}) \cos(kX_{H-L})) \quad (7)$$

Where:  $\mu$ : is the dynamic coulomb friction coefficient  
 $n$ : is the number of wave crests  
 $C_L$ : is the contact material stiffness

In the second part of USM model, the dynamic behavior of the rotor including the output torque generation and the angular velocity will be detailed. The output torque of USM ( $T_{USM}$ ) depends also on the surface contact variables ( $X_{H-L}$ ,  $X_s$ ) and the amplitude of the TW; it can be derived as [7]:

$$T_{USM} = \frac{2n\mu C_L \xi_{max} R_o}{k} (2\sigma(X_s) - \sigma(X_{H-L})) \quad (8)$$

$$\sigma(X) = \sin(kX) - kX_{H-L} \cos(kX_{H-L}) \quad (9)$$

The equation of rotational motion of the rotor is given by:

$$J_r \frac{d\Omega_{rotor}}{dt} = T_{USM} - T_{load} \quad (10)$$

Where:  $J_r$ : is the inertia of the rotor

$T_{load}$ : is the load torque

In this stage, the voltage phase difference value is included to determine the rotation direction and the corresponding generated torque. That means that negative, positive and around zero values of  $\phi$  are accepted by the model.

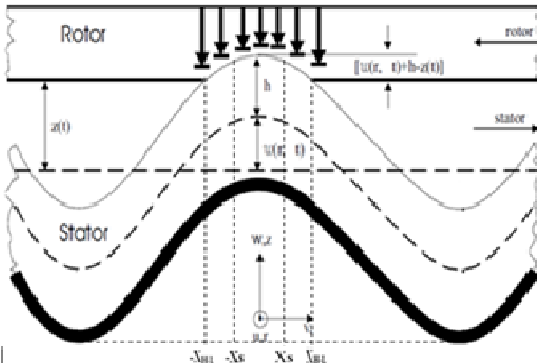


Fig.3: Section of the loaded stator undergoing bending deformations in the moving coordinate system

The performances of the proposed model are verified before applying the position control. From Fig.5 the resonance frequency of the motor can be easily deduced (40 kHz).

In figure 6, the two standing waves generated by each phase of the stator and the amplitude of the TW at the resonance

frequency ( $V_{rms}=100$ ,  $\phi=90^\circ$ ) are shown. From this model the parameters of the contact surface ( $X_{H-L}$ ,  $X_s$ ) and the vertical position of the rotor ( $z$ ) can be verified as shown in figure 7. The evolution of the angular velocity as function of the output torque is shown in figure 8 and one can see that the behavior given by the manufacturer datasheet is verified. In figure 9, load torque-speed characteristic at the frequency range between 40-41 kHz is presented.

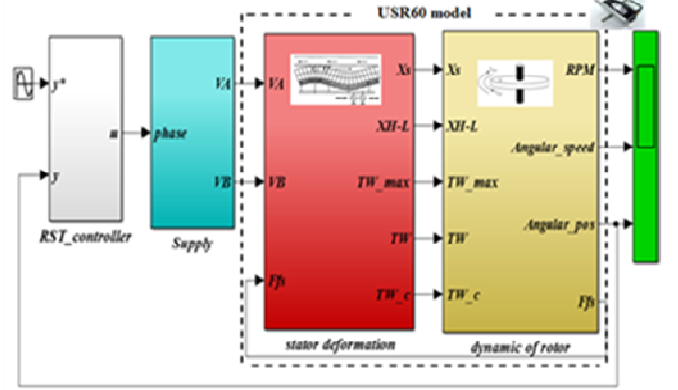


Fig.4: USR60 model width R-S-T position control

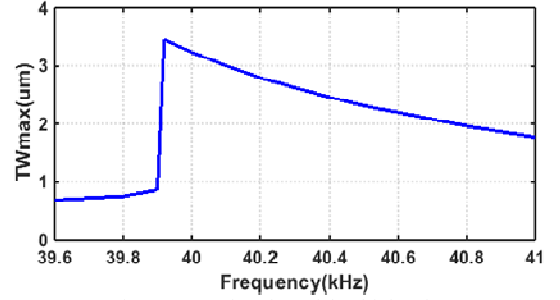


Fig.5: TW as function of the driving frequency

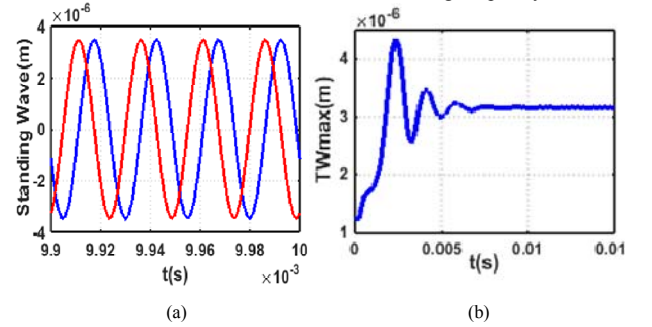


Fig.6: (a) Standing waves, (b) amplitude of TW(40kHz)

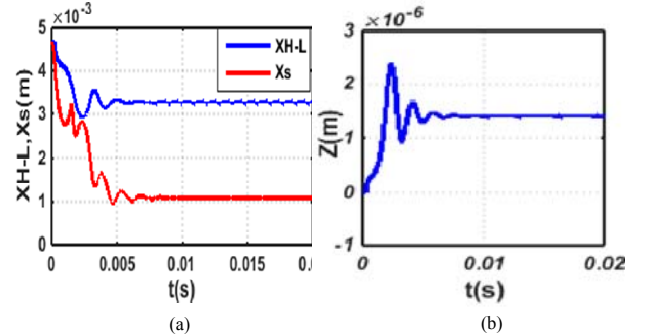


Fig.7: (a) Contact surface ( $X_{H-L}$ ,  $X_s$ ), (b) Vertical position( $Z$ )

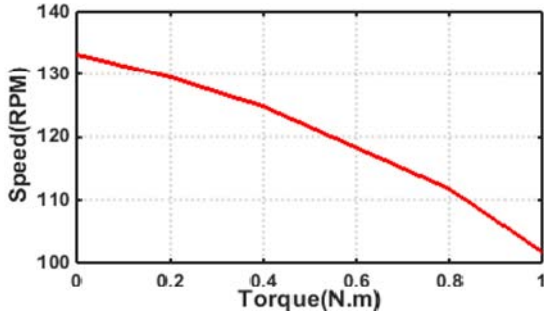


Fig.8: Angular velocity as function of the output torque

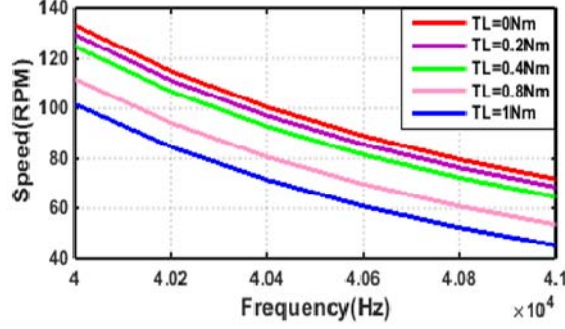


Fig.9: Effect of the load torque on the angular velocity

### III. RST BASED POSITION CONTROLLER DESIGN

In this section an accurate discrete-time RST position controller is presented. The goal of this controller is to ensure a precise regulation with large bandwidth. In parallel, the perturbation rejection will be validated using the supplementary degree of freedom of the RST controller.

#### A. RST controller synthesise

As mentioned above, USM can be controlled via the supply voltage amplitude, frequency, or phase difference. From short comparison between the three control variables results, it seems that the phase difference ( $\phi$ ) is the best choice to ensure a precise position control [14]. In addition, it gives easily the possibility to inverse the motor rotational direction that is requested in our application.

RST control consists of a discrete pole placement method based on the resolution of Diophantine equation [20]. As shown in figure 10, the RST control is composed by three discrete polynomials ( $R(z^{-1})$ ,  $S(z^{-1})$ , and  $T(z^{-1})$ ). The block  $B(z^{-1})/A(z^{-1})$  is the transfer function between the phase difference ( $\phi$ ) and angular position of the motor ( $y$ ). The eventual perturbations are represented by  $d_1$  and  $d_2$  in figure 10. The synthesis of RST control consists on the determination of those polynomial coefficients. We can write the control signal  $U(z^{-1})$  which represents the phase difference ( $\phi$ ) in real system as following:

$$U(z^{-1}) = \frac{T(z^{-1})}{S(z^{-1})} y^*(z^{-1}) - \frac{R(z^{-1})}{S(z^{-1})} y(z^{-1}) \quad (11)$$

The actual closed loop transfer function is given by:

$$\frac{y}{y^*} = \frac{B(z^{-1})T(z^{-1})}{A(z^{-1})S(z^{-1}) + B(z^{-1})R(z^{-1})} \quad (12)$$

As seen in equation (12), the polynomial  $T(z^{-1})$  appears only in the numerator giving the supplementary degree of freedom to this controller. The resolution methodology consist then in choosing reference closed loop system ( $H_m$ ) as function of the desired performance in term of bandwidth and damping factor:

$$H_m(z^{-1}) = \frac{B_m(z^{-1})}{A_m(z^{-1})} \quad (13)$$

To determine the coefficients of the polynomials  $R(z^{-1})$  and  $S(z^{-1})$ , we must resolve the Diophantine equation:

$$A_m(z^{-1}) = A(z^{-1})S(z^{-1}) + B(z^{-1})R(z^{-1}) \quad (14)$$

The polynomial  $T(z^{-1})$  can be deduced from the numerator of the reference closed loop system:

$$T(z^{-1}) = A_0 B_m(z^{-1}) \quad (15)$$

$A_0$  is a filter polynomial introduced to separate the dynamic regulation and the perturbation rejection.

The transfer function between error signal  $\varepsilon$  and the reference position is:

$$\frac{\varepsilon}{y^*} = 1 - \frac{y}{y^*} = 1 - H_m = \frac{A_m - B_m}{A_m} \quad (16)$$

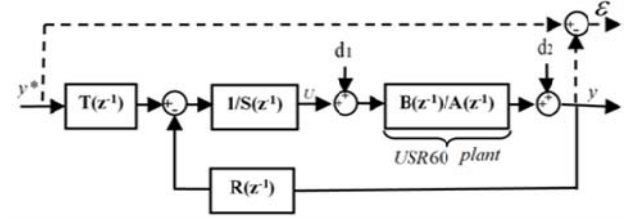


Fig.10: Discrete-time system controlled by an RST

In case of polynomial position references, the RST polynomials will also satisfy an auxiliary equation that includes the frequency of the reference signal. This polynomial position reference having the form  $y^*(t) = t^\beta$  and a Z-transform is  $y^*(z^{-1}) = y_1(z^{-1}) / (1 - z^{-1})^{\beta+1}$ .

To cancel the steady state error the term  $(1 - z^{-1})^{\beta+1}$  will divide  $A_m - B_m$ . This condition can be rewritten according to the final limit theorem by [20]:

$$A_m - B_m = (1 - z^{-1})^{\beta+1} L(z^{-1}) \quad (17)$$

Where;  $L(z^{-1})$  is a polynomial to be determined.

The sinusoidal reference waveform is a particular type of polynomial signals because the theorem of final limit can't be applied. From (16), we can write the magnitude of the frequency response of the error  $\varepsilon$  versus the input reference as following:

$$\left| \frac{\varepsilon}{y^*} \right|_{z=e^{j\omega T_s}} = \left| \frac{A_m - B_m}{A_m} \right|_{z=e^{j\omega T_s}} \quad (18)$$

Where:  $T_s$  is the sampling time.

Thus, to cancel the error at a given angular frequency  $\omega_0$ ; auxiliary equation must be satisfied:

$$\begin{aligned} A_m - B_m &= (1 - e^{j\omega_0 T_s} z^{-1})(1 - e^{-j\omega_0 T_s} z^{-1})L(z^{-1}) \\ &= (1 - 2\cos(\omega_0 T_s)z^{-1} + z^{-2})L(z^{-1}) \end{aligned} \quad (19)$$



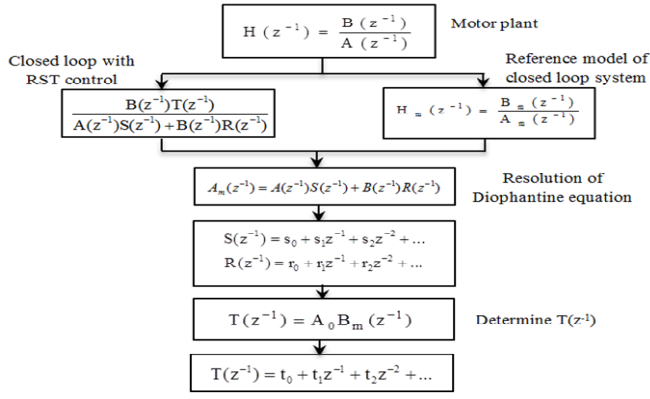


Fig.11: Flowchart of RST control synthesis

### B. RST based position control for USR60

The discrete-time RST control will be implemented now to validate the position control of USM. After the synthesis of the RST controller, it will be simulated with the developed model as shown in figure 4. As mentioned above, the position control signal is the voltages phase difference  $\phi$ . By applying a step of phase difference  $\phi$  and measuring the frequency response of the motor, the transfer function between the output angular position and the phase difference can be written as [15]:

$$\frac{y(s)}{\phi(s)} = \frac{K}{s(1 + \tau s)} \quad (20)$$

Where: the constant time  $\tau=0.0035s$  and the gain  $k=10.25$ .

The desired performance of the closed loop system in term of response time and damping factor of our application are respectively  $w=300\text{rad/s}$  and  $\xi=0.6$ . The synthesis of the regulator was done in discrete-time domain with sampling time  $T_s=1\text{ms}$ . So, the discrete plant model is given by:

$$G(z^{-1}) = \frac{B(z^{-1})}{A(z^{-1})} = \frac{0.0012 z^{-2} + 0.00133 z^{-1}}{0.75 z^{-2} - 1.75 z^{-1} + 1}$$

And the reference polynomial  $A_m$  can be determined:

$$A_m(z^{-1}) = 1 - 1.62z^{-1} + 0.69z^{-2}$$

By resolving the Diophantine equation (14), we obtain:

$$S(z^{-1}) = 1 + 0.049z^{-1} \quad R(z^{-1}) = 59.8 - 30.36z^{-1}$$

Sinusoidal position trajectory was tested firstly with an angular frequency  $w_0=10\text{rad/s}$ . The polynomial  $T(z^{-1})$  can be obtained by resolving the auxiliary equation (19):

$$L(z^{-1}) = 1 + 0.16z^{-1} \quad T(z^{-1}) = 162.1 - 132.6z^{-1}$$

Figure 12 shows the measured and reference sinusoidal position of USM with no load condition. The control signal ( $\phi$ ) and position error amount ( $\epsilon$ ) are given in figure 13. The pursuit of sinusoidal reference with angular rotation of  $90^\circ$  is ensured with an error of 2%. The addition of load torque has slightly affected the performance of the controller as shown in figure 14, where in the worst case ( $T_L=0.5\text{N.m}$ ) an amount of 6% of position error is obtained. Other position trajectories are tested with this controller as shown in figure 15 (triangular) and 16(square). Additional perturbations are added to the

measured position ( $d_2$ ) and to the control signal ( $d_1$ ) in order to validate the perturbation rejection capability of the controller. This robustness in front of perturbation is shown in figure 17. The closed loop performances of the controller in term of stability criteria (phase and gain margin) are verified as mentioned in table I.

TABLE I: RST-controller performance

bandwidth(rad/s)	Phase margin( $^\circ$ )	Gain margin(db)
300	55	6.48

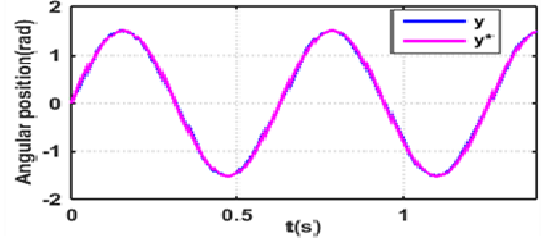


Fig.12: measured and reference sinusoidal position trajectory of USM

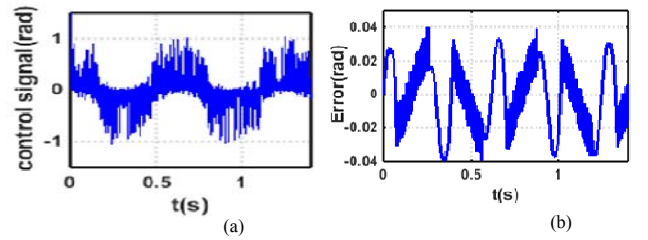
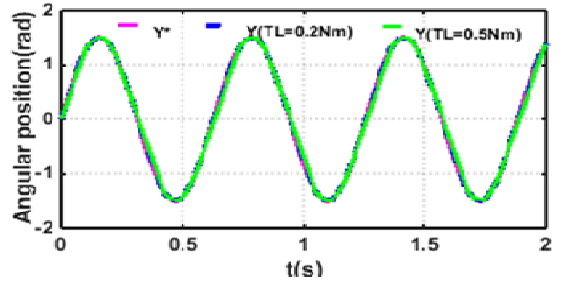

 Fig.13: (a) Control signal ( $\phi$ ); (b) error position ( $\epsilon$ )


Fig.14: Measured position with different load torque

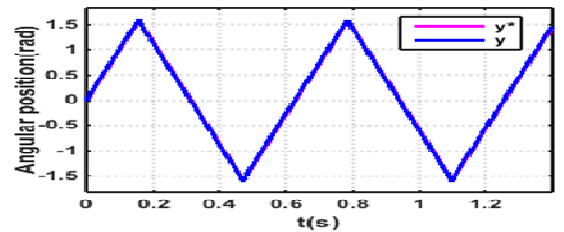


Fig.15: Measured and reference triangular position trajectory

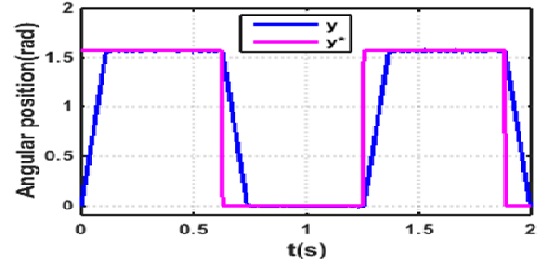


Fig.16: Measured and reference rectangular position trajectory

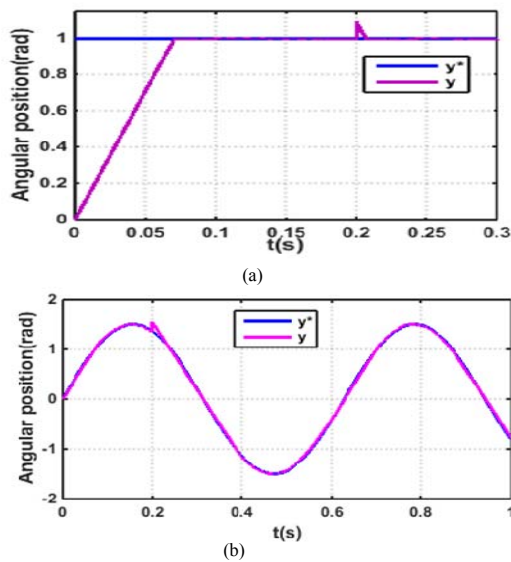


Fig.17: Closed loop response with perturbation injection: (a) step; (b) sinusoidal trajectory

#### IV. CONCLUSION

In this paper a model based control for rotary USM is proposed. This model is based on the electro-mechanical equations that describe the stator deformation and the rotor motion. It takes account the contact surface between stator and rotor and the nonlinearity behavior of the torque generation. This model is suitable for torque, speed, or position control and also via the supply voltage amplitude, frequency, or phase difference.

Discrete-time RST controller is developed then for the position control of USM. This controller gives the possibility to ensure separately the dynamic regulation and the perturbation rejection. Moreover, using the supplementary degree of freedom ( $T(z^{-1})$ ), the robustness of the controller in face of system dynamic variation and external perturbations can be achieved. Finally, the synthesis of the controller in discrete-time domain makes the hardware implementation simplest.

The USR60 model and the RST position controller are developed in MATLAB Simulink environment. The simulation results validate the performance of the proposed model coupled with RST position controller. The next step will be then the experimental validation of this controller with USR60 motor.

#### REFERENCES

- [1] T. Sashida, T. Kenjo, "An Introduction to Ultrasonic Motors" Oxford University Press, New York, 1993.
- [2] Ch.Zhao, "Ultrasonic Motors: Technologies and Applications" Science Press Beijing, 2011.
- [3] E.Bekiroglu, "Ultrasonic motors: Their models, drives, controls and applications," Journal of Electroceramics, Vol 20, pp 277-286, August 2008.
- [4] N.W.Hagood, A.J.McFarland, "Modeling of a piezoelectric rotary ultrasonic motor" IEEE Trans. Ultrason. Ferroelec. Freq. Control, 1995, 12(2): 210-221.

- [5] Maeno, T., T. Tsukimoto, and A. Miyake, "Finite-element analysis of the rotor/stator contact in a ring-type ultrasonic motor," Ultrasonics, Ferroelectrics and Frequency Control, IEEE Transactions on, 1992. 39(6): p. 668-674
- [6] P. Hagedorn, J. Wallaschek, "Travelling wave ultrasonic motors, Part I: Working principle and mathematical modeling of the stator," J Sound Vib 155(1), 31-46 (1992).
- [7] N. E. Gouti, "Hybrid modeling of a traveling wave piezoelectric motor," Ph.D. dissertation, Department of Control Engineering, Aalborg University, Denmark, 2000
- [8] S-A.Alsabbah, E.Mendes, Y.Bernard, "Derivation of Simplified Hybrid model and Speed Control for Travelling Wave Ultrasonic Motors," International Journal of Applied Electromagnetics and Mechanics, IJEM2003.France
- [9] F.Giraud, B.Semail, J-T.Audren, "Analysis and Phase Control of a Piezoelectric Traveling-Wave Ultrasonic Motor for Haptic Stick Application," IEEE Transaction on Industry Applications, Vol. 40, No. 6, 1541-1549 (2004).
- [10] N.W. Hagood, A.J. McFarland, "Modelling of a Piezoelectric Rotary Ultrasonic Motor," IEEE Trans. Ultrasonics. Ferroelectrics, Frequency Control 42(2), 210-224 (1995)
- [11] J. Maas, T. Schulte, and N. Frohliche, "Model-based control for ultrasonic motors," IEEE/ASME Transactions on Mechatronics, vol. 5, no. 2, pp. 165-180, June 2000.
- [12] A. Djoewahir, K. Tanaka, S. Nakashima, "Adaptive PSO-Based Self-Tuning PID Controller For Ultrasonic Motor," International Journal of Innovative Computing, Information and Control, Vol.9, pp.3903-3914, October 2013
- [13] K. Tanaka, Y. Wakasa, T. Akashi and M. Oka, "PI control adjusted by GA for ultrasonic motor," Electrical Engineering in Japan, vol.9, no.1, pp.663-668, 2009.
- [14] T. Senjyu, T. Kashiwagi, K. Uezato, "Position control of ultrasonic motors using MRAC and dead-zone compensation with fuzzy inference," IEEE Trans. Power Electron. 17(2), 265-272 (2002)
- [15] T. Senjyu, S. Yokada, Y. Gushiken, and K. Uezato, "Position control of ultrasonic motors using variable structure type adaptive control," 29th Annual IEEE Power Electronics Specialists Conference, vol. 2, pp. 1860-1866, 1998.
- [16] G.Bal, E. Bekiroglu, S.Demibras, I.Colak, "Fuzzy Logic Based DSP Controlled Servo Position Control for Ultrasonic Motor" Energy Convers.Manag, Vol.45, 3139-3153 (2004).
- [17] T. Senjyu, H. Miyazato, S. Yokoda, and K. Uezato, "Position control of ultrasonic motors using neural network," Proceedings of the IEEE International Symposium on Industrial Electronics, ISIE '96, vol. 1, pp. 368-373, 1996.
- [18] F-J.Lin, R-J.Wai, H-Hai.Yu, "Adaptive fuzzy-neural-network controller for ultrasonic motor drive using LLC resonant technique. IEEE Trans. on Ultrasonics, Ferroelectrics, and Frequency Control, 1999, pp 715-727.
- [19] F-J.Lin, R-J.Wai, H-Hai.Yu, "Fuzzy neural-network position controller for ultrasonic motor drive using push-pull DC-DC converter" IEEE Proceedings on Control Theory Application, 1998, 34(1): 363-368
- [20] E.Ostertag, E.Godoy, "RST-Controller Design for Sinewave References by Means of an Auxiliary Diophantine Equation," IEEE Conference on Decision and Control, pp 6905-6910, 2005